

Design of Localized High-Concentration Electrolytes via Donor Number

Juner Chen,[§] Han Zhang,[§] Mingming Fang,[§] Changming Ke,[§] Shi Liu,* and Jianhui Wang*



Cite This: *ACS Energy Lett.* 2023, 8, 1723–1734



Read Online

ACCESS |

Metrics & More

Article Recommendations

Supporting Information

ABSTRACT: Salt-concentrated electrolytes offer properties beyond conventional dilute electrolytes yet suffer from high cost and viscosity which hinder their practical applications. Introducing a secondary solvent as a diluent could reduce the salt content while maintaining the local solution structure of salt-concentrated electrolytes, giving rise to localized high-concentration electrolytes (LHCEs). Through a comprehensive investigation involving over 500 samples, we find that the dielectric constant of solvent, a widely used parameter for electrolyte design, does not serve as a useful screening criterion for diluents; instead, donor number (DN) is an effective design parameter to achieve LHCE structure—i.e., the primary solvent must have $\text{DN} > 10$ and the diluent must have $\text{DN} \leq 10$. Based on this simple rule, a new LHCE using low-cost *m*-fluorotoluene diluent is formulated, enabling high-voltage (>4.6 V) and wide-temperature (-40–100 °C) operation of lithium batteries.



Lithium-ion batteries, powering various portable electronics and electrically driven modes of transportation, are ubiquitous in our life, yet they are still far from an ideal energy storage device that meets the requirements of the ongoing, fast-developing mobile revolution due to their insufficient energy density and unsatisfying safety property. The capacity and safety limitations in current Li-ion batteries are considerably associated with the electrolyte. State-of-the-art Li-ion electrolytes have a general formula of 1 M (mol L⁻¹) solution of LiPF₆ salt dissolved in a mixed solvent of cyclic ethylene carbonate (EC) and linear carbonate esters. The LiPF₆ salt is chemically and thermally unstable, and the carbonate solvents are highly flammable, which strongly dictates a limited working voltage, a narrow operating temperature, and a high safety risk for the battery performance. Therefore, alternative electrolytes must be developed to replace these conventional electrolytes in the pursuit of high-energy-density and high-safety batteries.^{1,2}

Recently, salt-concentrated electrolytes have received great attention because of their superior properties beyond those of conventional dilute electrolytes.^{3–5} By simply increasing the salt concentration above a threshold (usually 3–5 M), all the solvent molecules and anions coordinate to Li⁺, resulting in a new solution structure with negligible free-state solvent molecules that is completely different from conventional dilute solutions wherein free-state solvent molecules take up the majority.^{6–11} This remarkable change of solution structure unique to the salt-concentrated electrolytes alters not only the

physicochemical properties but also the intrinsic electronic structure, contributing to a new design principle toward various LiPF₆-free and EC-free electrolytes with advanced properties for next-generation batteries, such as low flammability,^{11–13} wide electrochemical window,^{11,14,15} and suppression of dendrite formation and shuttle reactions.^{16–19} However, concentrated electrolytes suffer from high viscosity and high cost (salts are several times more expensive than solvents), which impede their practical applications.^{3–5}

A promising solution to this issue is the introduction of an appropriate diluent to form a so-called localized high-concentration electrolyte (LHCE), in which the diluent is miscible with the parent concentrated electrolyte but does not coordinate to Li⁺, such that the localized solution structure of the parent electrolyte is preserved. Enabled by the unique solution structure, LHCEs inherit advanced properties of concentrated electrolytes while exhibiting reduced viscosity and cost, as evidenced by extensive attempts to make sulfur cathode,^{20–22} lithium metal anode,^{23–26} and high-voltage lithium-ion batteries.^{27–30} Despite the remarkable progress, almost all the diluents reported are hydrofluoroethers that are

Received: January 1, 2023

Accepted: March 1, 2023

Published: March 10, 2023



ACS Publications

© 2023 American Chemical Society

Table 1. Information about the Studied Organic Solvents: DN Values,^a Dielectric Constants (ϵ), and Dipole Moments (μ)

Label	Solvents	DN	ϵ	μ	Label	Solvents	DN	ϵ	μ
1	Heptane (HPT)	0.0	1.9	0	19	1,4-Dioxane (DOA)	14.8	2.2	0.45
2	Cyclohexane (CYH)	0.0	2.0	0	20	Tetramethylene sulfone (SL)	14.8	42.0	4.68
3	Tetrachloromethane (CTC)	0.0	2.4	0	21	Propylene carbonate (PC)	15.1	64.6	4.94
4	Benzene (PhH)	0.1	2.3	0	22	Dimethyl carbonate (DMC)	15.2	3.0	0.93
5	Toluene (TOL)	0.1	2.4	0.31	23	Diethyl carbonate (DEC)	16.0	2.8	1.07
6	Hydrofluoroether (TTE)	1.9	6.2	-	24	Methyl propanoate (MP)	16.2	6.1	1.67
7	Dichlorobenzene (DCB)	2.0	4.9	1.68	25	Ethylene carbonate (EC)	16.4	90.8	4.51
8	Iodobenzene (IB)	4.0	4.6	1.71	26	Tetraglyme (G4)	16.6	7.7	-
9	Chloroform (TCM)	4.0	4.8	1.15	27	Ethyl Methyl Carbonate (EMC)	17.2	3.0	-
10	Cumene (iPB)	6.0	2.4	0.65	28	γ -Butyrolactone (γ -BL)	18.0	39.0	4.27
11	Phenetole (PhE)	8.0	4.3	1.41	29	Ethanol (ET)	19.2	24.6	1.66
12	Nitrobenzene (NB)	8.1	34.7	4.28	30	Monoglyme (DME)	20.0	7.2	1.71
13	Anisole (PhM)	9.0	4.4	1.36	31	Tetrahydrofuran (THF)	21.0	8.0	1.69
14	Mesitylene (MES)	10.0	2.3	0.10	32	1,3-dioxolane (DOL)	21.2	7.3	1.19
15	Phenol (PhOH)	11.0	12.4	1.55	33	Trimethyl phosphate (TMP)	23.0	20.6	2.82
16	Benzonitrile (BN)	13.0	25.7	4.28	34	Triethyl phosphate (TEP)	23.4	13.1	2.86
17	Triglyme (G3)	14.0	7.5	2.16	35	n-Amyl alcohol (nAA)	25.0	13.9	1.70
18	Acetonitrile (AN)	14.1	36.0	3.44	36	Dimethyl sulfoxide (DMSO)	29.8	46.4	4.10

^aDN values in this work are from ref 47.

even more expensive than the salt. Thereby, it is urgent to develop cheap diluents to reduce the cost of LHCEs.

However, finding an appropriate diluent to realize LHCEs relies mainly on the trial-and-error approach. In the research

field of electrolytes, the dielectric constant (ϵ) is widely regarded as an important parameter for solvents to regulate electrostatic interactions between solution components (e.g., ion–solvent, cation–anion, and solvent–solvent), thus dictat-

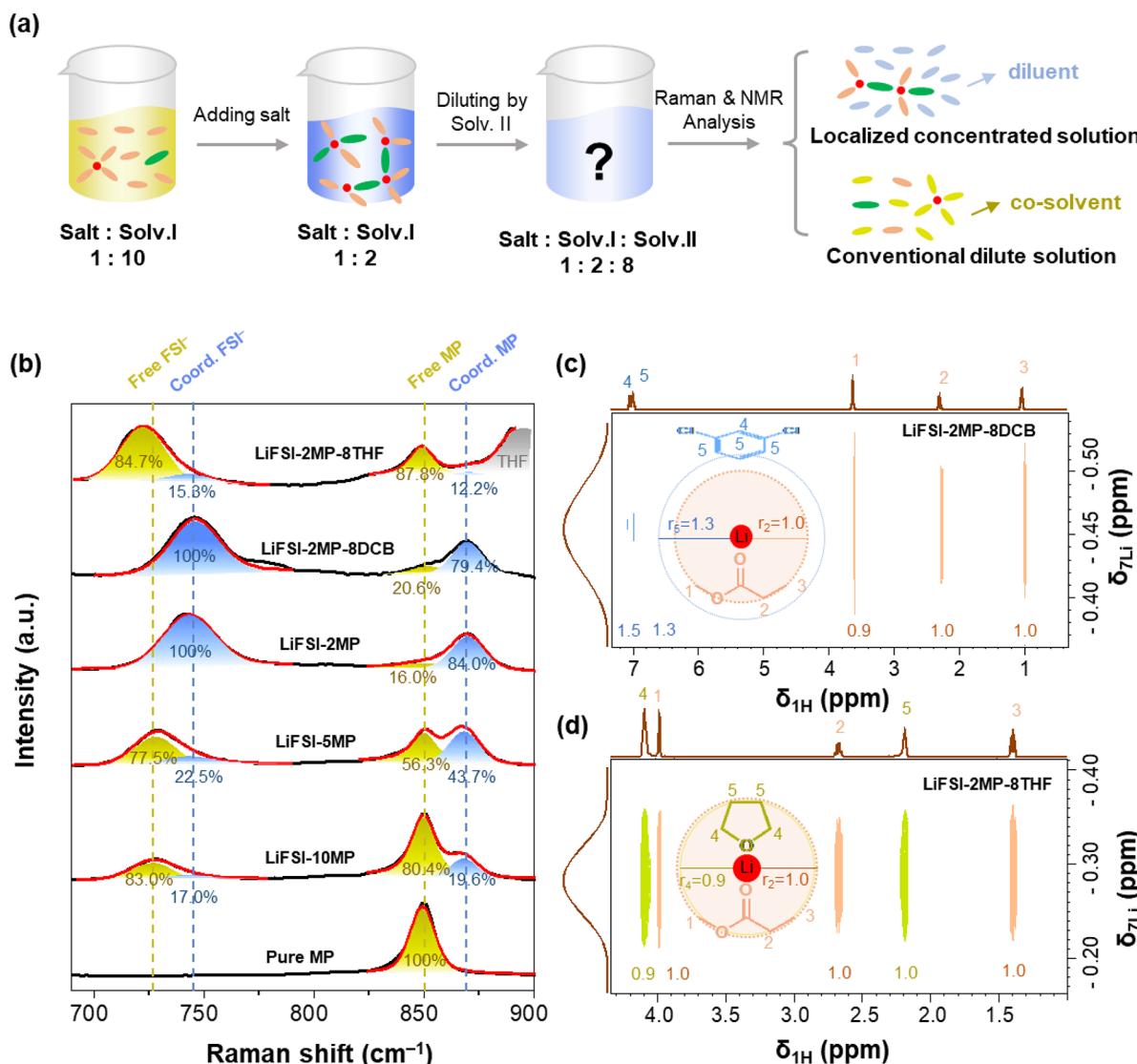


Figure 1. Representative demonstration of the preparation and characterization of LHCEs. (a) Schematic diagram of experimental procedures for electrolyte preparation and characterization. (b) Quantitative analysis of Raman spectra of a LiFSI-MP system with different salt concentrations and secondary solvents. It shows that the diluted solution of LiFSI-2MP-8DCB has a coordination structure similar to that of the parent concentrated solution of LiFSI-2MP, evidencing that the former is a LHCE and DCB is an eligible diluent, while the diluted solution of LiFSI-2MP-8THF has a coordination structure similar to that of the dilute solution of LiFSI-10MP, evidencing that THF is not a diluent but rather a co-solvent. (c, d) Quantitative analysis of the relative distances of Li⁺-Solv.I and Li⁺-Solv.II based on ¹H-⁷Li 2D HOESY NMR spectra of LiFSI-2MP-8DCB (c) and LiFSI-2MP-8THF (d). It indicates that DCB stays far away from Li⁺ and acts as a diluent, while THF stays close to Li⁺ and acts as a co-solvent, consistent with the Raman results.

ing the coordination environment of ions and the dissolution of salts.^{1,31–33} Taking the state-of-the-art Li-ion electrolyte as an example, high- ϵ EC is selected for multiple reasons: enhancing Li⁺-EC coordination, increasing the LiPF₆ solubility in the electrolyte, promoting the dissociation of solvated Li⁺, and enabling the formation of a protective film on the graphite anode.¹ According to this understanding, it is generally believed that a diluent should have a low ϵ , such that it cannot compete with primary solvent molecules to coordinate to Li⁺.^{23,28,34–37} This assumption looks valid at first sight because the most studied diluents, hydrofluoroethers, have a lower ϵ compared to many primary solvents (<6 vs 7–90). Additionally, some studies claimed that a diluent should have a lower polarity and/or donor ability.^{37–41} However, nearly all previous studies involved only a small number of samples (<10), leaving lots of counterexamples unexplored. As we will

discuss in this work, many solvents with ϵ , polarity (gauged by dipole moment, μ), and donor ability (gauged by donor number, DN) lower than those of the primary solvents participate considerably in the coordination to Li⁺, strongly deviating from those assumptions. More recently, solvating power was proposed as a measure to evaluate the relative coordination ability of solvents. The determination of a solvent's solvating power was reported through either NMR measurements⁴² or simulations.⁴³ However, the former relies on two internal references, with the reference–solvent interaction being ignored,⁴² while the latter lacks standard protocol.^{43–45} So far, the number of reported solvating power values is rather limited (<20), and they cannot be compared cross different literature sources (see Table S1). Besides, the Kamlet–Taft Lewis basicity was used to correlate with the solvation structures of LHCEs based on 14 samples.⁴⁶

However, the studied samples contained 40–50% free-state anions, which are not real LHCEs but rather conventional dilute solutions. Therefore, it is of fundamental importance to build up a reliable and convenient design principle for LHCEs.

In this work, we applied Raman and nuclear magnetic resonance (NMR) spectrometers to characterize the solution structures of over 500 electrolyte samples that had been diluted by 36 organics with different values of ϵ , μ , and DN. We specifically focus on the parameters ϵ , μ , and DN because they are most discussed and their values for many solvents are readily accessible from established databases. We found that the localized solution structure of the electrolyte does not show a meaningful correlation with ϵ and μ of the solvents but strongly correlates with a critical DN threshold. Specifically, an eligible diluent must have a $DN \leq 10$, independent of the type of salt anions and primary solvents. Our finding identifies the key factor determining the localized solution structure, which serves as a principle for fast screening of diluents for salt-concentrated electrolytes, thus contributing to the development of low-cost and high-performance LHCEs.

Preparation and Characterization of LHCEs. Lithium bis(fluorosulfonyl)imide (LiFSI) was selected as the salt in this study because it has a decent solubility in both polar and nonpolar solvents and is widely used for salt-concentrated electrolytes in the literature.⁴ A total of 36 organic solvents, including ethers, esters, nitriles, alcohols, aromatics, and alkanes, were used as primary solvents (termed as Solv.I) or diluent candidates (secondary solvents, termed as Solv.II) for electrolytes preparation (see Table S2 for product information); they have a wide range of ϵ (1–90), μ (0–5), and DN (0–30)⁴⁷ (shown in Table 1). Among them, 9 organics were selected as primary solvents (marked in blue in Table 1) because they can dissolve LiFSI in a high content to form concentrated electrolytes. Then, the concentrated electrolytes were mixed with 36 secondary solvents one by one to form diluted solutions with a LiFSI:Solv.I:Solv.II molar ratio of 1:2:8 (close to 1 M). After that, the chemical coordination environments of the primary solvent and FSI[−] anion in the diluted solutions were examined by Raman and/or NMR measurements. If the solution structural features of a diluted solution highly resemble those of the parent concentrated solution, we conclude that the diluted solution is a LHCE in which the introduced secondary solvent presents in the free state and is regarded as an eligible diluent. Otherwise, the introduced secondary solvent acts as a co-solvent that coordinates to Li⁺ like the primary solvent, breaking the solution structure of the parent concentrated solution (see Figure 1a for the experimental procedure). To demonstrate this method clearly, we take the LiFSI-methyl propanoate (MP) system as an example and show the structural analysis process.

As shown in the Raman spectra of LiFSI-MP solutions (Figure 1b), free-state MP molecules exhibit a C—O—C stretching vibration band centered at 850 cm^{−1} that shifts to 870 cm^{−1} when MP participates in Li⁺ coordination. Simultaneously, the peak center of the vibration band of the S—N—S group of FSI[−] shifts from 730 to 745 cm^{−1}, evidencing an enhanced interaction between FSI[−] and Li⁺ due to the fact that more FSI[−] anions coordinate to Li⁺ upon increasing the salt concentration. Therefore, four states of the MP molecule and FSI[−] anion can be recognized by their Raman character—“Free MP” (850 cm^{−1}), “Coord. MP” (870 cm^{−1}), “Free FSI[−]” (730 cm^{−1}), and “Coord. FSI[−]” (745 cm^{−1})—and the

corresponding contents of these four states can be easily evaluated by deconvoluting the Raman peaks (see Figure 1b).

In the same manner, we can quantitatively evaluate the solution structure for a diluted solution. Following the procedure shown in Figure 1a, we diluted the LiFSI-2MP solution with 36 organic solvents and measured their Raman spectra (see Figure S1). The results are summarized in Table S3 and can be categorized into two types: one type shows almost no shift in the Raman bands of both MP and FSI[−] after introduction of a secondary solvent, i.e., the contents of both Coord. MP and FSI[−] remain more than 75%, e.g., diluting with DCB in Figure 1b; the other type shows a significant shift in the Raman bands of both MP and FSI[−] and the reduction of the contents of both Coord. MP and FSI[−], e.g., diluting the LiFSI-2MP solution with 8 equiv of THF results in 75% of MP and 85% of FSI[−] changing from the coordinated state to the free state. Thereby, THF is a co-solvent for the LiFSI-2MP solution, while DCB is an eligible diluent.

Apart from Raman measurements, ¹H—⁷Li 2D heteronuclear Overhauser effect spectroscopy (2D HOESY) was also employed to identify the local coordination environment of a solution. A strong ¹H—⁷Li cross peak represents a close distance between H and Li, and vice versa.⁴⁸ As shown in Figure 1c, a strong ¹H (MP)—⁷Li cross peak and a weak ¹H (DCB)—⁷Li cross peak can be found for the diluted solution of LiFSI-2MP-8DCB, indicating that the DCB molecule stays farther away from Li⁺ as compared to the MP. In contrast, for the diluted solution of LiFSI-2MP-8THF, both cross peaks of ¹H (MP)—⁷Li and ¹H (THF)—⁷Li are equally strong, indicating both the MP and THF molecules stay close to Li⁺. The quantitative analysis of the 2D HOESY spectra can be found in Table S4. The above results suggest the DCB is a diluent and the THF is a co-solvent, consistent with the Raman results. For some samples, when the introduced secondary solvents have Raman bands overlapping with the anion or the primary solvent, it is difficult to evaluate the solution structure by deconvoluting the Raman spectra. In those cases, ¹H—⁷Li 2D HOESY spectra become the main measurement to identify a diluent.

To check if as-prepared diluted concentrated electrolytes inherit advanced physicochemical and electrochemical properties from the concentrated electrolyte, we carried out compatibility tests of lithium metal and graphite electrode with the electrolytes of LiFSI-10MP, LiFSI-2MP, LiFSI-2MP-8THF, and LiFSI-2MP-8DCB (Figure S2). As expected, the electrolyte of LiFSI-2MP-8THF, in which the local coordination structures of Li⁺ are similar to those in LiFSI-10MP, cannot stay stable with lithium metal and graphite electrode, confirming it behaves like a conventional diluent electrolyte. In contrast, the electrolyte of LiFSI-2MP-8DCB, which possesses a solution structure similar to that of the parent concentrated electrolyte of LiFSI-2MP, shows high compatibility with both lithium metal and graphite electrode, demonstrating that it does inherit the advanced properties of the concentrated electrolyte. Clearly, the above results prove that the localized solution structure of the electrolyte is critical for its physicochemical and electrochemical properties, and it is promising to develop cheap and high-performance LHCEs using conventionally cheap solvents as diluents. Therefore, it is urgent to find out the rule for screening appropriate diluents for LHCEs.

Solution Structure Dependence: ϵ vs μ vs DN. In previous reports, the solvation structure of lithium electrolyte

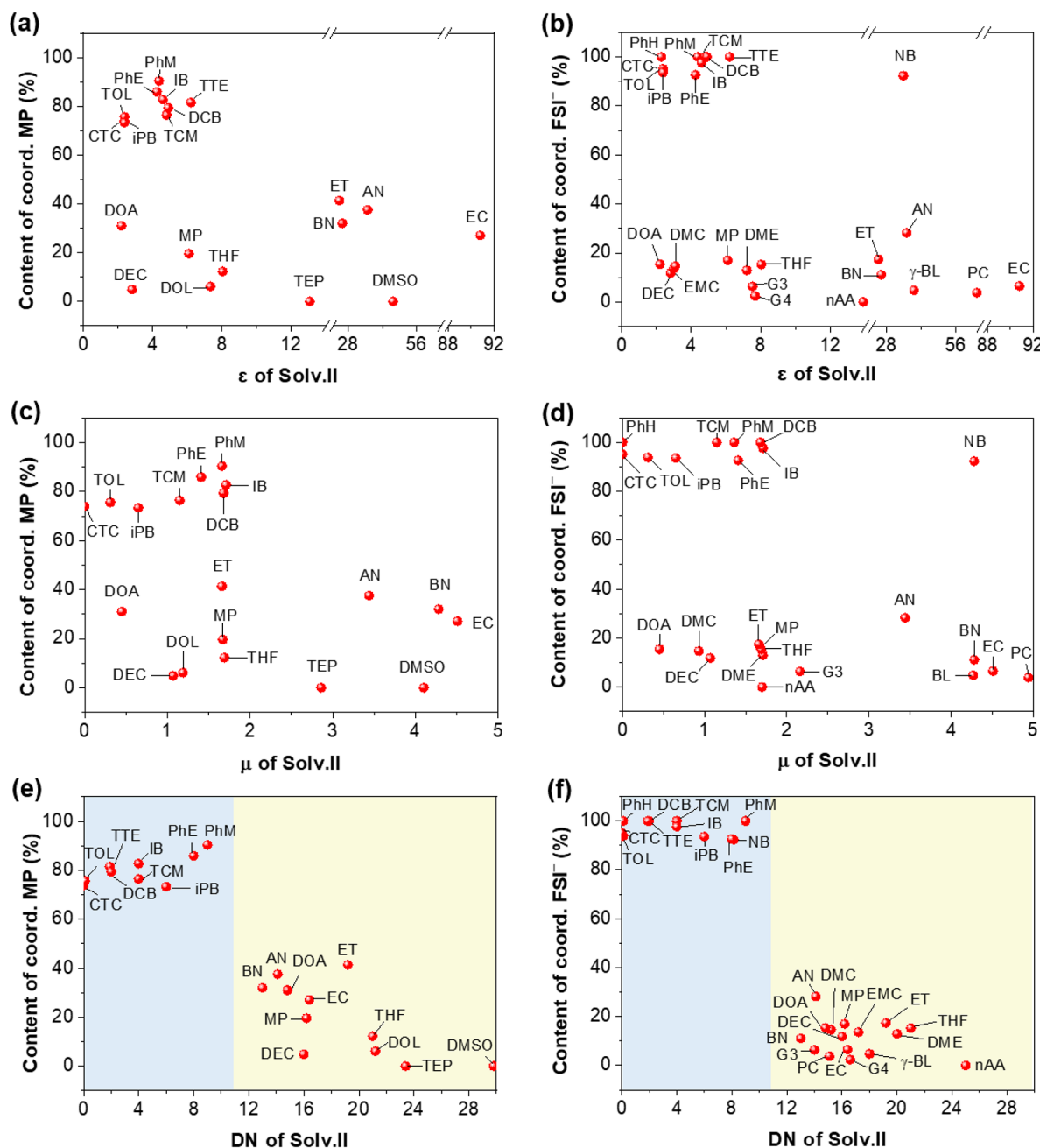


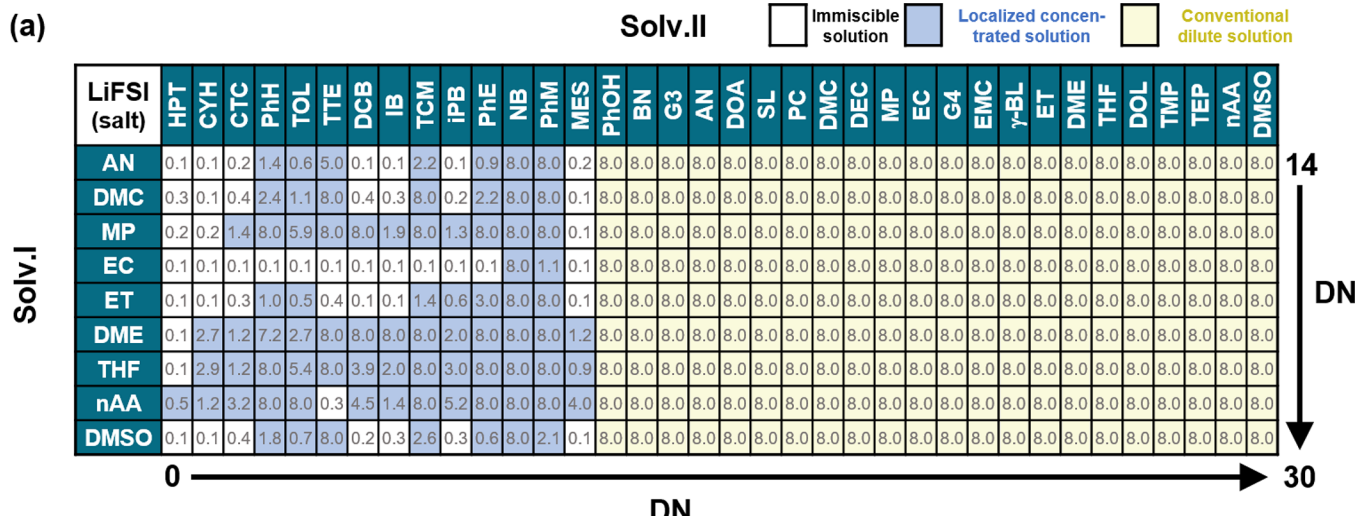
Figure 2. Correlation of coordinated species in the LiFSI-2MP-8[Solv.II] system with dielectric constant (ϵ) or dipole moment (μ) or DN of secondary solvents. (a, b) Content of coordinated MP molecules and FSI^- anions in the diluted solutions varying with ϵ of the introduced secondary solvents, respectively. (c, d) Content of coordinated MP molecules and FSI^- anions in the diluted solutions varying with μ of the introduced secondary solvents, respectively. (e, f) Content of coordinated MP molecules and FSI^- anions in the diluted solutions varying with DN of the introduced secondary solvents. No clear correlation can be found between the coordinated structure and ϵ or μ of the introduced secondary solvents. By contrast, a clear correlation can be observed between the coordinated structure and ϵ or μ of the introduced secondary solvents. For some diluted solutions, because the introduced secondary solvents have Raman bands overlapping with either those of MP or FSI^- , the corresponding contents of coordinated MP or FSI^- are difficult to evaluate and thus are not shown.

was usually associated with the dielectric constant of the solvent. This could be traced back to the studies on the classical electrolyte of 1 M LiPF_6 -EC-DMC, in which the two solvents, EC and DMC, have a large difference in ϵ (90.8 vs 3.0) but comparable DN values (16.4 vs 15.2). It is well known that the EC component contributes to a key solid-state electrolyte interphase that is essential for the reversible Li-intercalation/deintercalation of the graphite anode. This EC-derived interphase chemistry is usually associated with EC-Li⁺

solvation; the high ϵ of EC is regarded as the key factor responsible for such a coordination preference for EC over DMC to Li⁺.^{49,50} Accordingly, it is generally believed that the dielectric constant of the solvent has a great influence on the solvation structure as well as properties of a solution.

To find out the key factor for preparing a LHCE, we first studied the influence of dielectric constant on the solution structure of a diluted system of LiFSI-2MP-8[Solv.II]. The contents of coordinated MP and FSI^- in the diluted solutions

(a)



(b)

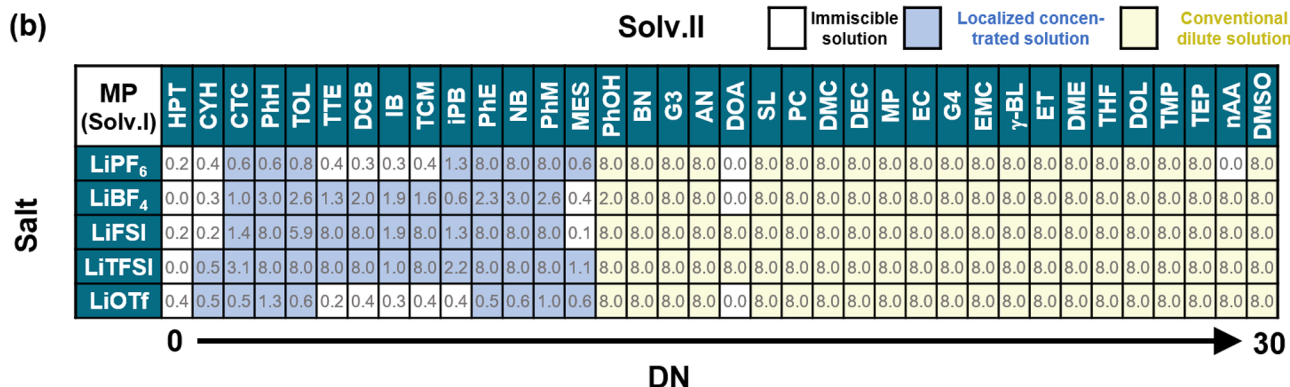


Figure 3. Coordination structures of the diluted concentrated electrolytes dependent on primary and secondary solvents as well as lithium salts. (a) Coordination structures of the $\text{LiFSI}-2[\text{Solv.I}]-8[\text{Solv.II}]$ system dependent on primary and secondary solvents. (b) Coordination structures of the $[\text{LiX}]-2\text{MP}-8[\text{Solv.II}]$ system dependent on lithium salts. In some cases, the introduction of secondary solvent leads to the solution's stratification. The numbers shown in the chart are the measured equivalent molar ratios of secondary solvents dissolved in the parent concentrated solution. A chart number less than 8 means that stratification occurs in the solution. A diluted solution with a too low content of secondary solvent (<0.5) is regarded as an immiscible solution (marked in white); that with a localized concentrated structure is marked in blue; the others are conventional dilute solutions (marked in olive green). For all the studied diluted solutions, the localized concentrated structure of the parent concentrated solution can be preserved only if the DN of the introduced secondary solvent is less than 10. This rule is valid for all 504 diluted samples of $[\text{LiX}]-2[\text{Solv.I}]-8[\text{Solv.II}]$, indicating it is independent of primary and secondary solvents and anions.

vs ϵ of Solv.II are plotted in Figure 2a and b, respectively. Surprisingly, we found that neither the content of coordinated MP nor that of FSI^- shows a significant correlation with $\epsilon_{\text{Solv.II}}$. For secondary solvents with $\epsilon < 6.1$ (MP), some diluted solutions have a high content of coordinated MP and FSI^- ($>70\%$), i.e., CTC ($\epsilon = 2.4$) and PhM ($\epsilon = 4.4$), while some samples show a low content of them ($<40\%$), i.e., DOA ($\epsilon = 2.2$) and DEC ($\epsilon = 2.8$). Additionally, the high content of coordinated FSI^- remains over 90% even after introducing a high- ϵ secondary solvent such as NB ($\epsilon = 34.7$), contradicting the common belief that a high- ϵ solvent can strongly coordinate to Li^+ and dissociate the lithium salts. Therefore, the dielectric constant of solvents, though being a widely used descriptor for electrolyte design, does not serve as a useful screening criterion for diluents of LHCEs.

Similarly, μ of Solv.II does not show a meaningful correlation with the solution structure of the diluted solutions either (see Figure 2c,d), whereas DN of Solv.II shows a strong correlation with the solution structure of the diluted solutions.

From Figure 2e,f, a clear boundary separating diluents and cosolvents (referred to as the “diluent boundary” hereinafter) can be observed in the $\text{LiFSI}-2\text{MP}-8[\text{Solv.II}]$ system: for secondary solvents with $\text{DN} \leq 9$ (PhM), the contents of coordinated MP and FSI^- remain $>70\%$ of those in the parent $\text{LiFSI}-2\text{MP}$ concentrated solution after diluting, indicating that these secondary solvents are eligible diluents, whereas for $\text{DN} \geq 13$ (BN), the contents of coordinated MP and FSI^- sharply decrease to $<40\%$, indicating that these secondary solvents act as co-solvents and the solution after dilution becomes a conventional dilute solution without a LHCE structural feature. It is noteworthy that the secondary solvents studied in this work include ethers, esters, nitriles, alcohols, aromatics, and alkanes, suggesting that the above finding is insensitive to the functional groups of organic solvents. Thereby, the coordination structure of the diluted solution is associated with the DN of the secondary solvents rather than ϵ and μ .

General Rule for Screening Diluent for LHCEs. The above results were obtained based on the system of LiFSI -

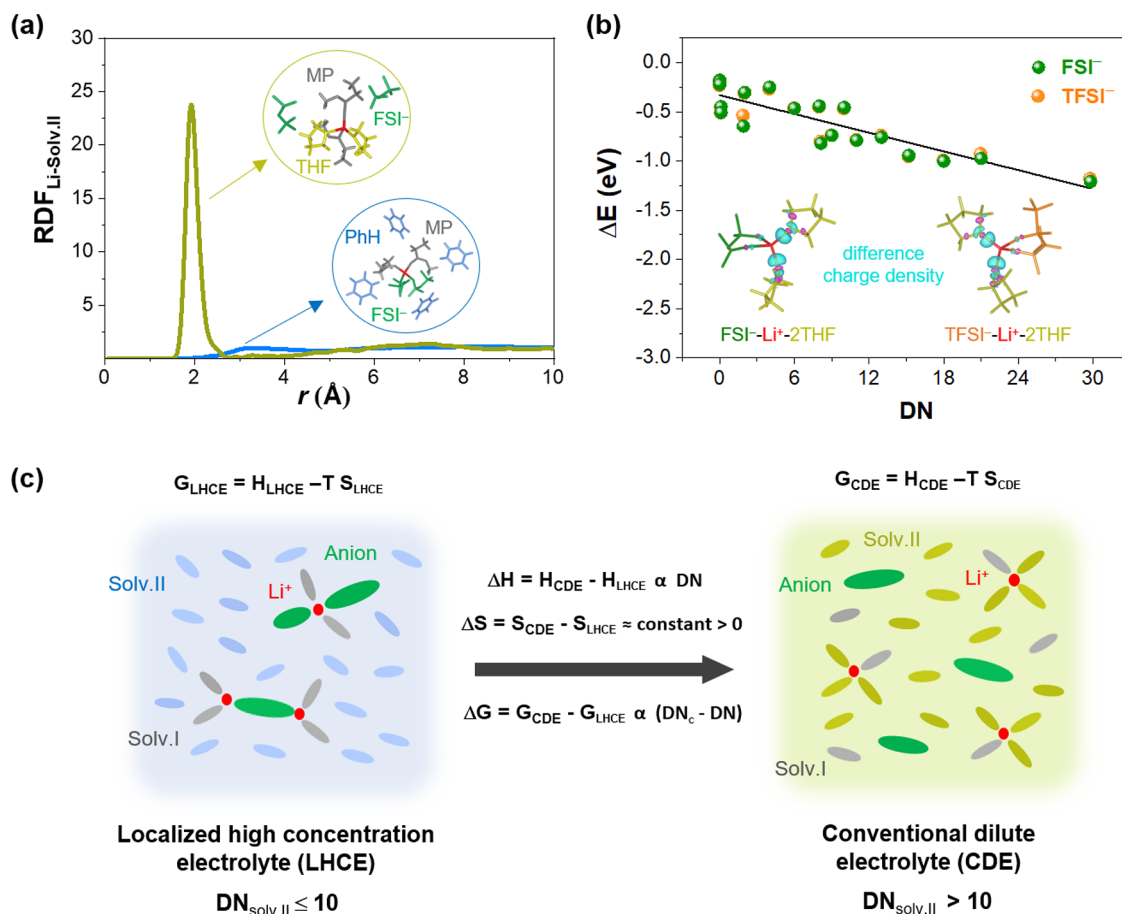


Figure 4. Quantum mechanical explanation of DN-based LHCE design principle. (a) Comparison of radial distribution functions (RDFs) of Li-Solv.II pairs and typical local coordination environment of Li⁺ in LiTFSI-2MP-2PhH and LiTFSI-2MP-2THF electrolytes from *ab initio* molecular dynamics. The calculation is performed in VASP using the PBE functional with periodic boundary conditions. (b) Linear scaling relationship between coordination energy ΔE of Solv.II with Li and DN values. The computation is carried out using the B3LYP functional with non-periodic boundary conditions. (c) Schematic illustration of the change in free energy for the transition from LHCE to CDE. DN_c represents the critical DN value (~10).

2MP-8[Solv.II] that used MP as the primary solvent. In a diluted concentrated electrolyte, the primary solvent molecule, the secondary solvent molecule, and the anion all can possibly participate in the coordination to Li⁺. Therefore, we further investigated the impacts of the primary solvent and the salt anion on the solution structures.

To study the effects of different primary solvents on the diluent boundary, eight other solvents with DN values over 14–30 were selected as the primary solvent for the diluted systems of LiTFSI-2[Solv.I]-8[Solv.II]. The solvents with DN < 11 were not used as the primary solvent because they cannot dissolve the LiTFSI salt at all (see Table 1). For all the nine concentrated solutions of LiTFSI-2[Solv.I] (including LiTFSI-2MP), the introduction of Solv.II led to either homogeneous solutions (miscible) or stratification (partially miscible or non-miscible). Figure 3a summarizes the results of all the 324 diluted samples. The values shown in the chart in Figure 3 are the actual equivalent molar ratios of Solv.II dissolved in the parent LiTFSI-2[Solv.I] solutions. For a value of <0.5 (too low solubility), the sample is regarded as an immiscible solution and does not undergo any further study. Otherwise, the sample undergoes Raman and/or NMR measurements for solution structure characterizations (Figures S3–S10). One might expect a secondary solvent with a DN value smaller than that of the primary solvent would be a diluent, thus leading to a

varied diluent boundary determined by the primary solvent. Surprisingly, Figure 3a shows that all the nine systems of LiTFSI-2[Solv.I]-8[Solv.II] have the same diluent boundary: the diluted samples keep LHCE structures when DN ≤ 10 but become conventional dilute solutions when DN > 13 .

We then studied the effects of salt anions on the diluent boundary. Five lithium salts (LiX) with different dissociation abilities, including LiTFSI, lithium hexafluorophosphate (LiPF₆), lithium tetrafluoroborate (LiBF₄), bis(trifluoromethylsulfonyl)imide (LiTFSI), and lithium triflate (LiOTf), were selected for a comparison study. Using MP as the primary solvent and the 36 secondary solvents mentioned above, we prepared 180 diluted solutions of LiX-2MP-8[Solv.II] and analyzed their coordination structures (Figures S11–S14). The results are summarized in Figure 3b. Clearly, it shows that regardless the anion type, the diluent boundary is fixed at DN ≈ 10 . From these results, we generalize three features regarding the diluent boundary: I) it has a DN value smaller than that of the primary solvent; II) it is fixed at DN ≈ 10 , independent of the types of primary solvents investigated here; III) it is insensitive to the anions of the Li salts. Hence, supported by thorough investigations involving over 500 samples, we identified a simple and general rule for screening a diluent for LHCEs: an eligible diluent must have a DN with a value no more than 10, independent of the types of organic

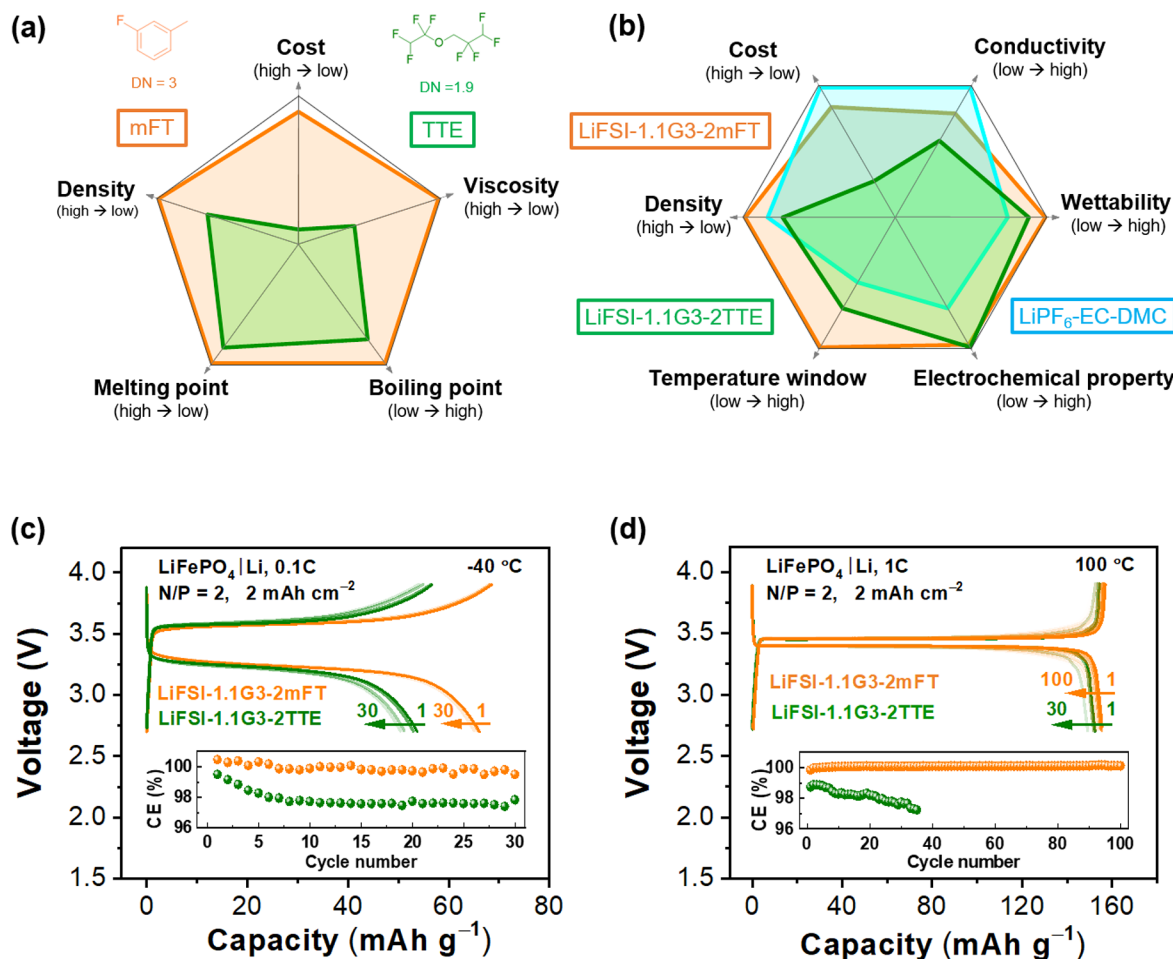


Figure 5. Comparison between the mFT and TTE diluents and their corresponding LHCEs. (a) Comparison of various physical properties between the mFT and TTE diluents. (b) Comparison of physical and electrochemical properties among the LHCEs of LiFSI-1.1G3-2mFT and LiFSI-1.1G3-2TTE and a commercial electrolyte of 1.0 M LiPF₆-EC-DMC (1:1 by vol.). (c, d) Comparison of charge–discharge cycling of the $\text{LiFePO}_4\text{||Li}$ full cells ($\text{N}/\text{P} = 2$, 2 mAh cm^{-2}) using the LHCEs of LiFSI-1.1G3-2mFT and LiFSI-1.1G3-2TTE at -40 and 100°C . The insets show the CEs dependent on cycle number. A 1C rate corresponds to 170 mA g^{-1} on the weight basis of the LiFePO_4 active material.

solvents or salt anions. Moreover, we plot the contents of coordinated species with respect to the DN of the secondary solvents based on the BF₃ scale and obtain nearly identical trends (Figure S15), confirming the robustness of our DN-based design principle.

Mechanistic Understanding of DN-Based Design Principle. To understand the origin of the diluent boundary, we explored the solution structures of a few representative electrolytes via *ab initio* molecular dynamic simulations (AIMD, see computational details in the Supporting Information). Here we focus on LiFSI-2MP-2THF and LiFSI-2MP-2PhH, as the DN of THF (28) is significantly different from that of PhH (0.1) while they have comparable dielectric constants ($\epsilon_{\text{THF}} = 8$ and $\epsilon_{\text{PhH}} = 2.3$). The AIMD snapshots of typical local environments of Li⁺ in these two electrolytes reveal that all low-DN PhH molecules remain as free-state solvents, whereas nearly all high-DN THF molecules participate in the coordination to Li⁺. This is further confirmed by the calculated radial distribution functions (RDFs) for the pairs of Li⁺ and secondary solvent molecules. As shown in Figure 4a, the RDF of Li⁺-THF has a pronounced peak at 2 Å, an indicator of strong interactions. In contrast, the RDFs of Li⁺-PhH are largely featureless, suggesting that PhH molecules distribute homogeneously in solution. We carried out addi-

tional modeling using Li salts of different anions (e.g., TFSI⁻, BF₄⁻, and OTf⁻), and the obtained RDFs (see Figure S16) all showed that the low-DN PhH is a diluent and the high-DN THF is a co-solvent regardless of the anion type, in agreement with experimental observations.

The solution structures revealed from AIMD hint that the DN value of Solv.II could be correlated with their coordination strength to Li⁺. Based on the local environments of Li⁺ identified from AIMD, we propose to use the interaction energy, defined as $\Delta E = \frac{1}{2}\{E[\text{LiX} \cdots 2\text{Solv.II}] - E[\text{LiX}] - 2E[\text{Solv.II}]\}$, to gauge the coordination ability of Solv.II, where $E[\text{LiX} \cdots 2\text{Solv.II}]$ is the energy of a molecular complex consisting of a Li⁺, an anion (X = FSI⁻ and TFSI⁻), and two coordinated Solv.II molecules (see inset in Figure 4b), $E[\text{LiX}]$ is the energy of an isolated anion–cation pair, and $E[\text{Solv.II}]$ is the energy of an isolated Solv.II molecule. As shown in Figure 4b, ΔE is almost linearly dependent on DN, supporting that DN is a good descriptor of the coordination ability. Moreover, for the same Solv.II molecule, the values of ΔE are insensitive to the types of anions (FSI⁻ and TFSI⁻). Such anion independence of ΔE can be understood as follows. The Li⁺–anion interaction is mostly of electrostatic (ionic) nature, such that the anion completely takes the 2s electron from the Li. In contrast, the interaction between Li⁺ and a solvent molecule is

a typical donor–acceptor coordination involving the lone pair of electrons from the solvent (e.g., O) and the empty 2s orbital of Li⁺. As Li⁺ has a highly concentrated charge, the energy of the 2s orbital is dictated by the Li⁺ core (nucleus plus 1s electrons) but less impacted by nearby anions, likely leading to an anion-independent Li⁺–solvent interaction. We also computed the differential charge densities of LiFSI-2THF and LiTFSI-2THF molecular complexes (Figure 4b inset), evidencing charge accumulations between Li⁺ and solvent molecules and the electron-sharing nature of the coordination. Notably, the two molecular complexes exhibit nearly identical differential charge density isosurfaces of the same value. Altogether, quantum mechanical calculations confirm that DN serves as a reliable and general measurement of the coordination ability of solvents to Li⁺ that is universal for various Li salts. The free energies of localized concentrated solutions and conventional dilute solutions, dependent on the DN of the secondary solvent, are proposed in Figure 4c. Given that the entropy change must occur during solvent mixing, the robust DN-based design principle may seem surprising, as DN is a descriptor of enthalpy change. Because the entropy of a solution is often dominated by the configurational contribution, it is reasonable to argue that the entropy change for a transition from LHCE to conventional dilute electrolyte (CDE) is positive and likely insensitive to the molecular details of solvents. We suggest that, for a given Solv.II, the free energy change for a transition from LHCE to CDE can be related to the difference between the DN_{Solv.II} and a critical DN value (DN_c, see detailed derivations in the Supporting Information), and the magnitude of DN_c is correlated with the entropy change. Nevertheless, due to the highly complex nature of the electrolytes, we believe that continued experimental and theoretical efforts are necessary for a full understanding of the DN-based design principle.

On the other hand, the failure of the ϵ -based design principle for LHCEs can be understood from the localized solution structure. The interaction between two charged ions separated by a distance r is described by Coulomb's law, $F = z_1 z_2 e^2 / 4\pi\epsilon_0 \epsilon r^2$, where z_1 and z_2 are the charges of the ions, respectively, ϵ_0 is the vacuum permittivity, and ϵ is the dielectric constant of the medium relative to vacuum. Apparently, in a dilute homogeneous solution with a high- ϵ solvent, ions would have a high probability of staying free at a given salt concentration and ion association would be less likely to occur due to the weaker Coulomb interactions. However, such a dielectric continuum solvation model is not applicable to salt-concentrated electrolytes, in which Li⁺ cations, anions, and solvent molecules are strongly bounded locally at the molecular level. It is the local interactions between salt ions and solvents that dictate the local solution structure, whereas the solvent can no longer be considered as a dielectric continuum. Similarly, the polarity of a solvent mainly scales with the strength of long-range dipole–dipole interactions between molecules. However, the electrostatic interaction is only one component of solvent–solute interactions, because there could exist short-range interactions due to charge transfer which are particularly important in LHCEs. As the DN value is directly derived from the enthalpy measurement that accounts for different types of solvent–solute interactions, we believe DN is a good descriptor of the solvent coordination strength to Li⁺ and is a more relevant solvent parameter to realize LHCEs.

A Low-Cost Diluent and Its Application in Li Batteries. Following the DN screening rule, it is easy to prepare LHCEs using a diluent solvent with DN < 10. As shown in Table 1, this kind of diluent solvent belongs mainly to aromatic or halogenated compounds. Among them, the fluorinated aromatic compounds could be good diluents owing to their wide electrochemical stability window, which is desired for a Li battery. Along this line, we selected *m*-fluorotoluene (*m*FT) as the diluent for LHCE based on its low cost, wide temperature window, and light weight (see Figure S17). As shown in Figure 5a and Table S5, compared with the widely studied diluent of 1,1,2,2-tetrafluoroethyl 2,2,3,3-tetrafluoropropyl ether (TTE), the cost, viscosity, and density of *m*FT are dramatically reduced by 88%, 60%, and 35%, respectively; meanwhile, the melting and boiling points are significantly extended to -111 and 116 °C, respectively. These features make the *m*FT-based LHCE (e.g., LiFSI-1.1G3-2mFT) considerably superior to the TTE-based one (e.g., LiFSI-1.1G3-2TTE) in various aspects of cost (\$26.0 vs \$79.9 kg⁻¹), wettability (5.180 vs 9.181 mPa·s), conductivity (8.30 vs 6.11 mS cm⁻¹), and density (1.17 vs 1.43 g cm⁻³) (see Figure 5b and Table S6). Besides those properties, the LiFSI-1.1G3-2mFT electrolyte has a wide electrochemical window of ~5 V, comparable with that of the LiFSI-1.1G3-2TTE electrolyte (Figure S18), which enables a high-voltage operation of the NCM811 and LiCoO₂ electrodes to 4.6 V and achieves a high capacity of ~220 mAh g⁻¹ (Figures S19 and S20). Moreover, the LiFSI-1.1G3-2mFT electrolyte demonstrates a profound advantage in wide-temperature applications: it enables a stable charge/discharge cycling of LiFePO₄|Li full cell (N/P = 2; 2.2 mAh cm⁻²) with an ultra-high Coulombic efficiency (CE) of 99.9% in an extremely wide temperature range from -40 to 100 °C, far exceeding to the LiFSI-1.1G3-2TTE electrolyte, whose CE falls to 98% in 10 cycles under such harsh conditions (see Figure 5c,d and Figure S21). This unprecedented wide-temperature performance could facilitate the development of an advanced high-energy-density battery system without using the bulky and heavy battery thermal management system (BTMS-free system).⁵¹ Finally, when comparing with the commercial electrolyte, the LiFSI-1.1G3-2mFT electrolyte also shows pronounced advantages besides the electrochemical performance (see Figure 5b). As the price of LiFSI salt is becoming close to that of LiPF₆, the cost of the *m*FT-based LHCEs could compete with the commercial electrolytes. Moreover, the density of the LiFSI-1.1G3-2mFT electrolyte (1.169 g cm⁻³) is decreased by ~12% as compared to commercial 1 M LiPF₆-EC-DMC (1:1 by vol) (1.324 g cm⁻³), which can contribute to an extra increase of battery energy density by 1–6%, given that the weight percentage of electrolyte in the whole battery is 10–50 wt%. Therefore, our developed LHCE shows a great promise for practical applications.

In summary, structural studies on hundreds of electrolytes reveal that the dielectric constant or polarity of a solvent is not a useful parameter to design LHCEs that possess nanoscale inhomogeneity. Instead, the DN, serving as a robust descriptor for the design of LHCEs, can be used to screen diluents: to achieve LHCE structure, the primary solvent must have DN > 10 and the diluent must have DN ≤ 10. The diluent boundary is fixed at DN ≈ 10, independent of the type of primary solvents and salt anions. First-principles density functional theory calculations confirmed that the Li–solvent interaction strength scales almost linearly with the DN value of the

solvent, while being insensitive to the anion type of the Li salts. Based on this simple rule, one can readily prepare electrolytes with the key feature of localized high-concentration solution structure that endows peculiar anion-derived electrode/electrolyte interphases, enlarging the space to explore high-performance electrolytes for next-generation batteries. In this work, a cheap mFT solvent was successfully selected as the diluent to form the mFT-based LHCE (LiFSI-1.1G3-2mFT). This low-cost LHCE enables not only a high-voltage operation of the NCM811 and LiCoO₂ electrodes to 4.6 V (~220 mAh g⁻¹) but also an extremely wide-temperature operation of the LiFePO₄|Li full cell (N/P = 2, 2 mAh cm⁻², CE 99.9% from -40 to 100 °C), far exceeding the LiFSI-1.1G3-2TTE electrolyte. Therefore, our findings show significant importance for both fundamental understanding and practical applications.

■ ASSOCIATED CONTENT

§ Supporting Information

The Supporting Information is available free of charge at <https://pubs.acs.org/doi/10.1021/acsenergylett.3c00004>.

Experimental methods (electrolyte and electrode preparation, Raman and NMR measurements, and electrochemical measurements), computational details, experimental data (Raman and NMR spectra, electrochemical properties for high-voltage cathodes (NCM811 and LiCoO₂) and low-voltage anodes (lithium metal and graphite)), a simple model to understand the DN criterion, and comparison between DN and other criteria for LHCEs ([PDF](#))

■ AUTHOR INFORMATION

Corresponding Authors

Jianhui Wang – Research Center for Industries of the Future, Westlake University, Hangzhou 310030, China; Key Laboratory of 3D Micro/Nano Fabrication and Characterization of Zhejiang Province, School of Engineering, Westlake University, Hangzhou 310030, China; Institute of Advanced Technology, Westlake Institute for Advanced Study, Hangzhou 310024, China; Department of Chemistry, Zhejiang University, Hangzhou 310027, China;
✉ orcid.org/0000-0002-4170-1132; Email: liushi@westlake.edu.cn

Shi Liu – Research Center for Industries of the Future, Westlake University, Hangzhou 310030, China; Key Laboratory for Quantum Materials of Zhejiang Province, School of Science, Westlake University, Hangzhou 310030, China; Institute of Natural Sciences, Westlake Institute for Advanced Study, Hangzhou 310024, China; ✉ orcid.org/0000-0002-8488-4848; Email: wangjianhui@westlake.edu.cn

Authors

Juner Chen – Key Laboratory of 3D Micro/Nano Fabrication and Characterization of Zhejiang Province, School of Engineering, Westlake University, Hangzhou 310030, China; Institute of Advanced Technology, Westlake Institute for Advanced Study, Hangzhou 310024, China

Han Zhang – Key Laboratory of 3D Micro/Nano Fabrication and Characterization of Zhejiang Province, School of Engineering, Westlake University, Hangzhou 310030, China;

Department of Chemistry, Zhejiang University, Hangzhou 310027, China

Mingming Fang – Key Laboratory of 3D Micro/Nano Fabrication and Characterization of Zhejiang Province, School of Engineering, Westlake University, Hangzhou 310030, China

Changming Ke – Key Laboratory for Quantum Materials of Zhejiang Province, School of Science, Westlake University, Hangzhou 310030, China; Institute of Natural Sciences, Westlake Institute for Advanced Study, Hangzhou 310024, China

Complete contact information is available at:
<https://pubs.acs.org/10.1021/acsenergylett.3c00004>

Author Contributions

§ J.C., H.Z., M.F., and C.K. contributed equally to this work. J.W. and J.C. designed the experiments. J.C. and H.Z. carried out the experiments of electrolyte preparation and solution structure characterizations. M.F. carried out the experiments of electrochemical performances. S.L. directed the computation. S.L. and C.K. designed and performed the DFT-MD simulations. J.W. conceived and led the project. All authors contributed to the discussion and the manuscript preparation.

Notes

The authors declare no competing financial interest.

■ ACKNOWLEDGMENTS

This work was supported by Research Center for Industries of the Future (RCIF) and Key Laboratory of 3D Micro/nano Fabrication and Characterization of Zhejiang Province at Westlake University, Westlake Education Foundation, National Natural Science Foundation of China (Grant No. 21975207), Zhejiang Provincial Natural Science Foundation of China (Grant No. LQ21B030006), and Postdoctoral Science Foundation of Zhejiang Province (Grant No. ZJ2020079). The calculations and NMR measurements were performed at Westlake HPC Center and Instrumentation and Service Center for Molecular Sciences, respectively. The authors thank Prof. Wenjie Dai for his useful suggestions on the manuscript and Dr. Xiaohuo Shi for his assistance in NMR data interpretation.

■ REFERENCES

- (1) Xu, K. Nonaqueous liquid electrolytes for lithium-based rechargeable batteries. *Chem. Rev.* **2004**, *104*, 4303–4417.
- (2) Xu, K. Electrolytes and interphases in Li-ion batteries and beyond. *Chem. Rev.* **2014**, *114*, 11503–11618.
- (3) Zheng, J. M.; Lochala, J. A.; Kwok, A.; Deng, Z. Q. D.; Xiao, J. Research Progress towards Understanding the Unique Interfaces between Concentrated Electrolytes and Electrodes for Energy Storage Applications. *Adv. Sci.* **2017**, *4*, 1700032.
- (4) Yamada, Y.; Wang, J.; Ko, S.; Watanabe, E.; Yamada, A. Advances and issues in developing salt-concentrated battery electrolytes. *Nat. Energy* **2019**, *4*, 269–280.
- (5) Borodin, O.; Self, J.; Persson, K. A.; Wang, C. S.; Xu, K. Uncharted Waters: Super-Concentrated Electrolytes. *Joule* **2020**, *4*, 69–100.
- (6) Jeong, S. K.; Inaba, M.; Iriyama, Y.; Abe, T.; Ogumi, Z. Electrochemical intercalation of lithium ion within graphite from propylene carbonate solutions. *Electrochim. Solid State Lett.* **2003**, *6*, A13–A15.
- (7) Yoshida, K.; Nakamura, M.; Kazue, Y.; Tachikawa, N.; Tsuzuki, S.; Seki, S.; Dokko, K.; Watanabe, M. Oxidative-stability enhancement and charge transport mechanism in glyme-lithium salt equimolar complexes. *J. Am. Chem. Soc.* **2011**, *133*, 13121–13129.

- (8) Yamada, Y.; Furukawa, K.; Sodeyama, K.; Kikuchi, K.; Yaegashi, M.; Tateyama, Y.; Yamada, A. Unusual stability of acetonitrile-based superconcentrated electrolytes for fast-charging lithium-ion batteries. *J. Am. Chem. Soc.* **2014**, *136*, 5039–5046.
- (9) Suo, L. M.; Borodin, O.; Gao, T.; Olguin, M.; Ho, J.; Fan, X. L.; Luo, C.; Wang, C. S.; Xu, K. "Water-in-salt" electrolyte enables high-voltage aqueous lithium-ion chemistries. *Science* **2015**, *350*, 938–943.
- (10) Lin, R.; Ke, C. M.; Chen, J.; Liu, S.; Wang, J. H. Asymmetric donor-acceptor molecule-regulated core-shell-solvation electrolyte for high-voltage aqueous batteries. *Joule* **2022**, *6*, 399–417.
- (11) Wang, J.; Yamada, Y.; Sodeyama, K.; Chiang, C. H.; Tateyama, Y.; Yamada, A. Superconcentrated electrolytes for a high-voltage lithium-ion battery. *Nat. Commun.* **2016**, *7*, 12032.
- (12) Wang, J. H.; Yamada, Y.; Sodeyama, K.; Watanabe, E.; Takada, K.; Tateyama, Y.; Yamada, A. Fire-extinguishing organic electrolytes for safe batteries. *Nat. Energy* **2018**, *3*, 22–29.
- (13) Zeng, Z. Q.; Murugesan, V.; Han, K. S.; Jiang, X. Y.; Cao, Y. L.; Xiao, L. F.; Ai, X. P.; Yang, H. X.; Zhang, J. G.; Sushko, M. L.; Liu, J. Non-flammable electrolytes with high salt-to-solvent ratios for Li-ion and Li-metal batteries. *Nat. Energy* **2018**, *3*, 674–681.
- (14) Alvarado, J.; Schroeder, M. A.; Zhang, M. H.; Borodin, O.; Gobrogge, E.; Olguin, M.; Ding, M. S.; Gobet, M.; Greenbaum, S.; Meng, Y. S.; Xu, K. A carbonate-free, sulfone-based electrolyte for high-voltage Li-ion batteries. *Mater. Today* **2018**, *21*, 341–353.
- (15) Ko, S.; Yamada, Y.; Yamada, A. An overlooked issue for high-voltage Li-ion batteries: Suppressing the intercalation of anions into conductive carbon. *Joule* **2021**, *5*, 998–1009.
- (16) Suo, L. M.; Hu, Y. S.; Li, H.; Armand, M.; Chen, L. Q. A new class of Solvent-in-Salt electrolyte for high-energy rechargeable metallic lithium batteries. *Nat. Commun.* **2013**, *4*, 1481.
- (17) Qian, J. F.; Henderson, W. A.; Xu, W.; Bhattacharya, P.; Engelhard, M.; Borodin, O.; Zhang, J. G. High rate and stable cycling of lithium metal anode. *Nat. Commun.* **2015**, *6*, 6362.
- (18) Suo, L. M.; Xue, W. J.; Gobet, M.; Greenbaum, S. G.; Wang, C.; Chen, Y. M.; Yang, W. L.; Li, Y. X.; Li, J. Fluorine-donating electrolytes enable highly reversible 5-V-class Li metal batteries. *Proc. Natl. Acad. Sci. U.S.A.* **2018**, *115*, 1156–1161.
- (19) Fan, X. L.; Chen, L.; Ji, X.; Deng, T.; Hou, S. Y.; Chen, J.; Zheng, J.; Wang, F.; Jiang, J. J.; Xu, K.; Wang, C. S. Highly Fluorinated Interphases Enable High-Voltage Li-Metal Batteries. *Chem* **2018**, *4*, 174–185.
- (20) Dokko, K.; Tachikawa, N.; Yamauchi, K.; Tsuchiya, M.; Yamazaki, A.; Takashima, E.; Park, J. W.; Ueno, K.; Seki, S.; Serizawa, N.; Watanabe, M. Solvate Ionic Liquid Electrolyte for Li-S Batteries. *J. Electrochem. Soc.* **2013**, *160*, A1304–A1310.
- (21) Pang, Q.; Shyamsunder, A.; Narayanan, B.; Kwok, C. Y.; Curtiss, L. A.; Nazar, L. F. Tuning the electrolyte network structure to invoke quasi-solid state sulfur conversion and suppress lithium dendrite formation in Li-S batteries. *Nat. Energy* **2018**, *3*, 783–791.
- (22) Liu, T.; Li, H. J.; Yue, J. M.; Feng, J. N.; Mao, M. L.; Zhu, X. Z.; Hu, Y. S.; Li, H.; Huang, X. J.; Chen, L. Q.; Suo, L. M. Ultralight Electrolyte for High-Energy Lithium-Sulfur Pouch Cells. *Angew. Chem., Int. Ed.* **2021**, *60*, 17547–17555.
- (23) Ren, X. D.; Chen, S. R.; Lee, H.; Mei, D. H.; Engelhard, M. H.; Burton, S. D.; Zhao, W. G.; Zheng, J. M.; Li, Q. Y.; Ding, M. S.; et al. Localized High-Concentration Sulfone Electrolytes for High-Efficiency Lithium-Metal Batteries. *Chem* **2018**, *4*, 1877–1892.
- (24) Cao, X.; Ren, X. D.; Zou, L. F.; Engelhard, M. H.; Huang, W.; Wang, H. S.; Matthews, B. E.; Lee, H.; Niu, C. J.; Arey, B. W.; et al. Monolithic solid-electrolyte interphases formed in fluorinated orthoformate-based electrolytes minimize Li depletion and pulverization. *Nat. Energy* **2019**, *4*, 796–805.
- (25) Fan, X. L.; Ji, X.; Chen, L.; Chen, J.; Deng, T.; Han, F. D.; Yue, J.; Piao, N.; Wang, R. X.; Zhou, X. Q.; et al. All-temperature batteries enabled by fluorinated electrolytes with non-polar solvents. *Nat. Energy* **2019**, *4*, 882–890.
- (26) Piao, N.; Ji, X.; Xu, H.; Fan, X. L.; Chen, L.; Liu, S. F.; Garaga, M. N.; Greenbaum, S. C.; Wang, L.; Wang, C. S.; He, X. M. Countersolvent Electrolytes for Lithium-Metal Batteries. *Adv. Energy Mater.* **2020**, *10*, 1903568.
- (27) Doi, T.; Shimizu, Y.; Hashinokuchi, M.; Inaba, M. Dilution of Highly Concentrated LiBF₄/Propylene Carbonate Electrolyte Solution with Fluoroalkyl Ethers for 5-V LiNi_{0.5}Mn_{1.5}O₄Positive Electrodes. *J. Electrochem. Soc.* **2017**, *164*, A6412–A6416.
- (28) Takada, K.; Yamada, Y.; Yamada, A. Optimized Nonflammable Concentrated Electrolytes by Introducing a Low-Dielectric Diluent. *ACS Appl. Mater. Interfaces* **2019**, *11*, 35770–35776.
- (29) Jia, H. P.; Zou, L. F.; Gao, P. Y.; Cao, X.; Zhao, W. G.; He, Y.; Engelhard, M. H.; Burton, S. D.; Wang, H.; Ren, X. D.; et al. High-Performance Silicon Anodes Enabled By Nonflammable Localized High-Concentration Electrolytes. *Adv. Energy Mater.* **2019**, *9*, 1900784.
- (30) Zhang, X.; Zou, L.; Xu, Y.; Cao, X.; Engelhard, M. H.; Matthews, B. E.; Zhong, L.; Wu, H.; Jia, H.; Ren, X.; et al. Advanced Electrolytes for Fast-Charging High-Voltage Lithium-Ion Batteries in Wide-Temperature Range. *Adv. Energy Mater.* **2020**, *10*, 2000368.
- (31) Reichardt, C.; Welton, T. *Solvents and Solvent Effects in Organic Chemistry*, 4th updated and expanded ed.; Wiley-VCH Verlag GmbH: Weinheim, 2010; pp 52–56.
- (32) Bogle, X.; Vazquez, R.; Greenbaum, S.; Cresce, A.; Xu, K. Understanding Li(+)–Solvent Interaction in Nonaqueous Carbonate Electrolytes with ¹⁷O NMR. *J. Phys. Chem. Lett.* **2013**, *4*, 1664–1668.
- (33) Yao, N.; Chen, X.; Shen, X.; Zhang, R.; Fu, Z. H.; Ma, X. X.; Zhang, X. Q.; Li, B. Q.; Zhang, Q. An Atomic Insight into the Chemical Origin and Variation of the Dielectric Constant in Liquid Electrolytes. *Angew. Chem., Int. Ed.* **2021**, *60*, 21473–21478.
- (34) Ding, J. F.; Xu, R.; Yao, N.; Chen, X.; Xiao, Y.; Yao, Y. X.; Yan, C.; Xie, J.; Huang, J. Q. Non-Solvating and Low-Dielectricity Cosolvent for Anion-Derived Solid Electrolyte Interphases in Lithium Metal Batteries. *Angew. Chem., Int. Ed.* **2021**, *60*, 11442–11447.
- (35) Jia, H.; Zhang, X. H.; Xu, Y. B.; Zou, L. F.; Kim, J. M.; Gao, P. Y.; Engelhard, M. H.; Li, Q. Y.; Niu, C. J.; Matthews, B. E.; et al. Toward the Practical Use of Cobalt-Free Lithium-Ion Batteries by an Advanced Ether-Based Electrolyte. *ACS Appl. Mater. Interfaces* **2021**, *13*, 44339–44347.
- (36) Wu, Q.; Tang, X.; Qian, Y.; Duan, J. D.; Wang, R.; Teng, J. H.; Li, J. Enhancing the Cycling Stability for Lithium-Metal Batteries by Localized High-Concentration Electrolytes with 2-Fluoropyridine Additive. *ACS Appl. Energy Mater.* **2021**, *4*, 10234–10243.
- (37) Pham, T. D.; Lee, K. K. Simultaneous Stabilization of the Solid/Cathode Electrolyte Interface in Lithium Metal Batteries by a New Weakly Solvating Electrolyte. *Small* **2021**, *17*, 2100133.
- (38) Ueno, K.; Murai, J.; Ikeda, K.; Tsuzuki, S.; Tsuchiya, M.; Tataro, R.; Mandai, T.; Umebayashi, Y.; Dokko, K.; Watanabe, M. Li⁺ Solvation and Ionic Transport in Lithium Solvate Ionic Liquids Diluted by Molecular Solvents. *J. Phys. Chem. C* **2016**, *120*, 15792–15802.
- (39) Zheng, J. M.; Chen, S. R.; Zhao, W. G.; Song, J. H.; Engelhard, M. H.; Zhang, J. G. Extremely Stable Sodium Metal Batteries Enabled by Localized High-Concentration Electrolytes. *ACS Energy Lett.* **2018**, *3*, 315–321.
- (40) Zheng, J.; Ji, G.; Fan, X.; Chen, J.; Li, Q.; Wang, H.; Yang, Y.; DeMella, K. C.; Raghavan, S. R.; Wang, C. High-Fluorinated Electrolytes for Li–S Batteries. *Adv. Energy Mater.* **2019**, *9*, 1803774.
- (41) He, M. X.; Li, X.; Yang, X. F.; Wang, C. H.; Zheng, M. H. L.; Li, R. Y.; Zuo, P. J.; Yin, G. P.; Sun, X. L. Realizing Solid-Phase Reaction in Li–S Batteries via Localized High-Concentration Carbonate Electrolyte. *Adv. Energy Mater.* **2021**, *11*, 2101004.
- (42) Moon, J.; Kim, D. O.; Bekaert, L.; Song, M.; Chung, J.; Lee, D.; Hubin, A.; Lim, J. Non-fluorinated non-solvating cosolvent enabling superior performance of lithium metal negative electrode battery. *Nat. Commun.* **2022**, *13*, 4538.
- (43) Singh, S.; Nanda, R.; Dorai, K. Structural and dynamical aspects of PEG/LiClO₄ in solvent mixtures via NMR spectroscopy. *Magn. Reson. Chem.* **2019**, *57*, 412–422.

- (44) Morita, M.; Asai, Y.; Yoshimoto, N.; Ishikawa, M. A Raman spectroscopic study of organic electrolyte solutions based on binary solvent systems of ethylene carbonate with low viscosity solvents which dissolve different lithium salts. *J. Chem. Soc. Faraday Trans.* **1998**, *94*, 3451–3456.
- (45) Xu, K.; Lam, Y. F.; Zhang, S. S.; Jow, T. R.; Curtis, T. B. Solvation sheath of Li^+ in nonaqueous electrolytes and its implication of graphite/electrolyte interface chemistry. *J. Phys. Chem. C* **2007**, *111*, 7411–7421.
- (46) Yang, L.; Xiao, A.; Lucht, B. L. Investigation of solvation in lithium ion battery electrolytes by NMR spectroscopy. *J. Mol. Liq.* **2010**, *154*, 131–133.
- (47) Christian, L.; Jean-François, G. *Lewis Basicity and Affinity Scales: Data and Measurement*; John Wiley & Sons; 2010; pp 75–77.
- (48) Johnson, L.; Li, C. M.; Liu, Z.; Chen, Y. H.; Freunberger, S. A.; Ashok, P. C.; Praveen, B. B.; Dholakia, K.; Tarascon, J. M.; Bruce, P. G. The role of LiO_2 solubility in O_2 reduction in aprotic solvents and its consequences for $\text{Li}-\text{O}_2$ batteries. *Nat. Chem.* **2014**, *6*, 1091–1099.
- (49) Gupta, A.; Bhargav, A.; Manthiram, A. Highly Solvating Electrolytes for Lithium-Sulfur Batteries. *Adv. Energy Mater.* **2019**, *9*, 1803096.
- (50) Baek, M.; Shin, H.; Char, K.; Choi, J. W. New High Donor Electrolyte for Lithium-Sulfur Batteries. *Adv. Mater.* **2020**, *32*, No. e2005022.
- (51) Wang, J. H.; Zheng, Q. F.; Fang, M. M.; Ko, S. J.; Yamada, Y.; Yamada, A. Concentrated Electrolytes Widen the Operating Temperature Range of Lithium-Ion Batteries. *Adv. Sci.* **2021**, *8*, 2101646.

□ Recommended by ACS

Design Criteria of Dilute Ether Electrolytes toward Reversible and Fast Intercalation Chemistry of Graphite Anode in Li-Ion Batteries

Dawei Xia, Feng Lin, et al.

FEBRUARY 13, 2023

ACS ENERGY LETTERS

[READ ↗](#)

Solvent versus Anion Chemistry: Unveiling the Structure-Dependent Reactivity in Tailoring Electrochemical Interphases for Lithium-Metal Batteries

Digen Ruan, Xiaodi Ren, et al.

FEBRUARY 17, 2023

JACS AU

[READ ↗](#)

Modifying the Interface between the Solvated Ionic Liquid Electrolyte and Positive Electrode to Boost Lithium-Ion Battery Performance

Jun Deng, Taro Hitosugi, et al.

SEPTEMBER 01, 2022

ACS APPLIED ENERGY MATERIALS

[READ ↗](#)

A Competitive Solvation of Ternary Eutectic Electrolytes Tailoring the Electrode/Electrolyte Interphase for Lithium Metal Batteries

Wanbao Wu, Jiaheng Zhang, et al.

AUGUST 30, 2022

ACS NANO

[READ ↗](#)